J|A|C|S ARTICLES

Published on Web 03/01/2010

CopK from *Cupriavidus metallidurans* CH34 Binds Cu(I) in a Tetrathioether Site: Characterization by X-ray Absorption and NMR Spectroscopy

Géraldine Sarret,[†] Adrien Favier,[‡,§,||] Jacques Covès,[‡,§,||] Jean-Louis Hazemann,[⊥] Max Mergeay,[#] and Beate Bersch*[,‡,§,||]

Environmental Geochemistry Group, LGIT, UMR 5559, Université Joseph Fourier and CNRS, BP 53, 38041 Grenoble, France, Institut de Biologie Structurale—J.P. Ebel, UMR 5075, CNRS, F-38027 Grenoble, France, CEA, F-38054 Grenoble, France, UJF, F-38000 Grenoble, France, Institut Néel, CNRS, 38042 Grenoble Cedex 9, France, and Molecular and Cellular Biology, Belgian Center for Nuclear Energy, SCK•CEN, B-2400 Mol, Belgium

Received October 2, 2009; E-mail: beate.bersch@ibs.fr

Abstract: *Cupriavidus metallidurans* CH34 is a bacterium that is resistant to high metal concentrations in the environment. Increased copper resistance is associated with the *cop* cluster on the large plasmid pMOL30 that is composed of at least 21 genes. The *copK* gene encodes a 74 residue periplasmic protein whose expression is strongly upregulated in the presence of copper. CopK was previously shown to cooperatively bind Cu(I) and Cu(II) in distinct, specific sites. The solution structure of Cu(I)−CopK and the characterization of the Cu(I) site by X-ray absorption spectroscopy and NMR are reported here. EXAFS spectra are in agreement with a tetrathioether Cu(I) site, providing so far unique spectral information on a 4S-coordinated Cu(I) in a protein. The methionine residues forming the Cu(I) site, M28, M38, M44, and M54, are identified by NMR. We propose the chemical shift of the methionine C^{ε} as a new and sensitive probe for the detection of Cu(I) bound to thioether groups. The solution structure of Cu(I)−CopK demonstrates that Cu(I) binding induces a complete structural modification with the disruption of the second β-sheet and a rotation of the C-terminal part of nearly 180° around a hinge formed by asparagine 57. This conformational change is directly related to the loss of the dimer interface and most probably to the formation of the Cu(II) site involving histidine 70. The solution structure of Cu(I)−CopK therefore provides the molecular basis for the understanding of the Cu(I)/Cu(II) binding cooperativity.

Introduction

Cupriavidus metallidurans CH34 is a β-proteobacterium initially isolated from sediments of a zinc decantation basin in Belgium.[1,2] It represents an important model for the study of heavy metal resistance, as it can survive at millimolar concentrations of multiple heavy metals.[3−5] The genome of *C. metallidurans* CH34 contains two large plasmids, pMOL28 and pMOL30, that carry gene clusters coding for numerous heavy metal resistance proteins.[6,7] Microarray analysis showed that the 21 genes of the *cop* determinant, which is located on plasmid pMOL30, are highly upregulated in the presence of Cu(II).[8] This *cop* cluster comprises the basic *copSRABCD* operon, which is homologous to the plasmid-located *pco*/*cop* operons previously characterized in *Escherichia coli* and *Pseudomonas syringae* pv tomato,[9−11] as well as *copF*, encoding a P1-ATPase involved in the detoxification of the cytoplasm.[12] However, the function of the other Cop proteins remains still unclear, but it is thought that the ensemble of these proteins is required for resistance to the elevated copper concentrations found in highly polluted industrial biotopes.

Recently, we determined the solution structure of apo-CopK, a periplasmic low molecular weight protein that is highly expressed in the presence of Cu(II) and showed that this protein could bind up to 2 mol equiv of copper.[13] Later, Wedd's group demonstrated that CopK bound Cu(I) and Cu(II) in two distinct

[†] Université Joseph Fourier and CNRS.
[‡] Institut de Biologie Structurale—J.P. Ebel.
[§] CEA.
[||] UJF.
[⊥] Institut Néel.
[#] Belgian Center for Nuclear Energy.

(1) Vandamme, P.; Coenye, T. *Int. J. Syst. Evol. Microbiol.* **2004**, *54*, 2285–2289.
(2) Mergeay, M. In *Bacterial Stress Responses*; Storz, G., Hengge-Aronis, R., Eds.; ASM Press: Herndon, VA, 2000; pp 403−414.
(3) Mergeay, M.; Monchy, S.; Vallaeys, T.; Auquier, V.; Benotmane, A.; Bertin, P.; Taghavi, S.; Dunn, J.; van der Lelie, D.; Wattiez, R. *FEMS Microbiol. Rev.* **2003**, *27*, 385–410.
(4) Nies, D. H.; Rehbein, G.; Hoffmann, T.; Baumann, C.; Grosse, C. *J Mol. Microbiol. Biotechnol.* **2006**, *11*, 82–93.
(5) von Rozycki, T.; Nies, D. H. *Antonie Van Leeuwenhoek* **2009**, *96*, 115–139.
(6) Monchy, S.; Benotmane, M. A.; Janssen, P.; Vallaeys, T.; Taghavi, S.; van der Lelie, D.; Mergeay, M. *J. Bacteriol.* **2007**, *189*, 7417–25.
(7) Van Houdt, R.; Monchy, S.; Leys, N.; Mergeay, M. *Antonie Van Leeuwenhoek* **2009**, *96*, 205–226.
(8) Monchy, S.; Benotmane, M. A.; Wattiez, R.; van Aelst, S.; Auquier, V.; Borremans, B.; Mergeay, M.; Taghavi, S.; van der Lelie, D.; Vallaeys, T. *Microbiology* **2006**, *152*, 1765–1776.
(9) Rensing, C.; Grass, G. *FEMS Microbiol. Rev.* **2003**, *27*, 197–213.
(10) Cooksey, D. A. *FEMS Microbiol. Rev.* **1994**, *14*, 381–386.
(11) Adaikkalam, V.; Swarup, S. *Can. J. Microbiol.* **2005**, *51*, 209–216.
(12) Monchy, S.; Vallaeys, T.; Bossus, A.; Mergeay, M. *Int. J. Environ. Anal. Chem.* **2006**, *86*, 677–692.

 10.1021/ja9083896

metal sites with an unprecedented binding cooperativity.[14] They also determined the crystal structures of dimeric apo and Cu(I)-bound forms of this protein. Comparison of these structures indicated no significant structural change upon binding of Cu(I).[14] This was in contradiction with NMR data that clearly demonstrated dimer dissociation related to Cu(I) binding.[13,14] Consequently, the authors suggested that intermolecular hydrogen bonding in the crystal dominated the effect of Cu(I) binding and imposed the dimeric structure of the apo protein. In order to better characterize the molecular basis of the Cu(I)/Cu(II)-binding cooperativity, we determined the solution structure of Cu(I)−CopK that is presented here.

NMR structure determination of metalloproteins requires the identification of the residues forming the metal binding site. Different spectroscopic techniques such as UV−vis absorption, EPR, or X-ray absorption (XAS) spectroscopies can be applied according to the metal and its ligands, in order to identify the atoms contributing to the ligand shell. However, in most cases, these techniques do not provide any sequence specific information. On the other hand, NMR has extensively been used for the sequence-specific identification of metal binding sites in proteins, mostly based on observed backbone chemical shift variations.[15−17] Unambiguous information will only be obtained in the case of local structural perturbations and unless there are not several possible metal−ligands in spatial proximity of the supposed metal site. CopK, for instance, contains five conserved methionines in positions 26, 28, 38, 44, and 54 and undergoes major structural changes related to dimer dissociation upon interaction with Cu(I). Identification of the Cu(I) ligands is therefore not possible unless using a specific probe that directly detects the modification of the electronic structure due to the presence of Cu(I). In the present study, we demonstrate that the methionine C^{ε} chemical shift can be used for the unambiguous identification of methionine residues involved in Cu(I) coordination. The Cu(I) site of Cu(I)−CopK has also been characterized by XAS, and the solution structure of Cu(I)−CopK has been determined combining experimental information from NMR as well as from XAS.

Material and Methods

Sample Preparation for NMR and XAS. The CopK protein was obtained as described previously.[13] Cu(I)-bound CopK for NMR and XAS studies was prepared by subsequently adding 10 mol equiv of sodium ascorbate, pH 8.0, prepared by titration of ascorbic acid with NaOH and 1 mol equiv of $CuCl_2$ dissolved in water. NMR samples were prepared in a glovebox and placed in an NMR tube hermetically closed with a rubber septum. They were found to be stable for at least 2 weeks. For the XAS experiment, the protein was concentrated to a final concentration of 2.7 mM in 50 mM ammonium acetate, pH 6.8, containing 15% glycerol in order to avoid formation of crystal ice; 100 μL of the Cu(I)−CopK sample was transferred directly after preparation to a PEEK homemade five-cell sample holder with a Kapton window and flash-frozen in liquid nitrogen.

A sample of ^{13}C,^{15}N-labeled Cu(I)Cu(II)−CopK was prepared by adding 2 mol equiv of $CuCl_2$ to a 2 mM CopK sample in the presence of 50 mM ammonium acetate and 20 mM NH_2OH.[14] Incubation was followed by gel filtration on a NAP-5 column (GE Healthcare), equilibrated with 50 mM MOPS buffer, pH 6.8. Sample was eluted in 1 mL of the same buffer and used for NMR spectroscopy without additional concentration. Final sample concentration could be estimated to 0.8 mM according to signal intensity in an ^{1}H,^{15}N-HSQC spectrum that demonstrated that Cu(I)Cu(II)−CopK had been obtained as expected.

X-ray Absorption Spectroscopy (XAS). XAS measurements were carried out at the European Synchrotron Radiation Facility (ESRF, Grenoble, France), which was operating with a ring current of 150−200 mA. Cu K-edge XAS spectra were collected on the BM30B (FAME) beamline using a Si(220) double crystal monochromator with dynamic sagittal focusing. The photon flux was on the order of 10^{12} photons per second and the spot size was 300 μm horizontal × 100 μm vertical.[18]

The sample holder was loaded in a helium cryostat with temperature set to 10 K during data collection. The spectra were collected in fluorescence mode by measuring the Cu Kα fluorescence with a 30-element solid-state Ge detector (Canberra). Twelve scans of 40 min each were averaged. Data from each detector channel were inspected for glitches or dropouts before inclusion in the final average.

Energy calibration was achieved by measuring a copper foil for the Cu edge and assigning the first inflection point of the Cu foil spectrum to 8980.3 eV.

Data analysis was performed using the IFEFFIT package,[19] including ATHENA for the data extraction and ARTEMIS for the shell fitting. X-ray absorption near edge structure (XANES) spectra were background-corrected by a linear regression through the pre-edge region and a cubic spline through the postedge region and normalized to the edge jump. The spectrum for Cu(I)−CopK was compared qualitatively to the reference spectra for Cu(I)−Met and Cu(II)−Met provided by D'Angelo et al.[20] For the extraction of the extended X-ray absorption fine structure (EXAFS) part, E_0 was defined at the half-height of the absorption edge step. k^3-weighted EXAFS spectra were Fourier transformed over the k range 3.7−12.9 Å^{-1} using a Kaiser−Bessel window ($\alpha = 2.5$). Fits were performed on the Fourier filtered spectra over the $R + \Delta R$ range 0.9−3.4 Å. Theoretical amplitude and phase shift functions were calculated with the ab initio code FEFF 7.0[21] using the refined structure of Cu(I)−CopK as well as structures for simple Cu−organic complexes from the Cambridge Structural Database (http://www.ccdc.cam.ac.uk/products/csd/). ConQuest software[22] was used to search for typical Cu−S distances in Cu(I)−3S and Cu(I)−4S small compounds in CSD.

NMR Spectroscopy. All NMR experiments were performed on Varian VNMRS 600 or 800 spectrometers equipped with triple-resonance (^{1}H, ^{13}C, ^{15}N) cryoprobes and shielded z-gradients. The experiments were acquired at 25 °C with typical sample concentrations between 1.0 and 2.0 mM. All chemical shifts were referenced with respect to the H_2O signal at 4.77 ppm (pH 6.8, 25 °C) relative to DSS, using the $^{1}H/X$ frequency ratios of the zero point according to Markley et al.[23]

(13) Bersch, B.; Favier, A.; Schanda, P.; van Aelst, S.; Vallaeys, T.; Coves, J.; Mergeay, M.; Wattiez, R. *J. Mol. Biol.* **2008**, *380*, 386–403.
(14) Chong, L. X.; Ash, M. R.; Maher, M. J.; Hinds, M. G.; Xiao, Z.; Wedd, A. G. *J. Am. Chem. Soc.* **2009**, *131*, 3549–3564.
(15) Wernimont, A. K.; Huffman, D. L.; Finney, L. A.; Demeler, B.; O'Halloran, T. V.; Rosenzweig, A. C. *J. Biol. Inorg. Chem.* **2003**, *8*, 185–194.
(16) Banci, L.; Bertini, I.; Ciofi-Baffoni, S.; Katsari, E.; Katsaros, N.; Kubicek, K.; Mangani, S. *Proc. Natl. Acad. Sci. U.S.A.* **2005**, *102*, 3994–3999.
(17) Kittleson, J. T.; Loftin, I. R.; Hausrath, A. C.; Engelhardt, K. P.; Rensing, C.; McEvoy, M. M. *Biochemistry* **2006**, *45*, 11096–11102.
(18) Proux, O.; Nassif, V.; Prat, A.; Ulrich, O.; Lahera, E.; Biquard, X.; Menthonnex, J. J.; Hazemann, J. L. *J. Synchrotron Radiat.* **2006**, *13*, 59–68.
(19) Ravel, B.; Newville, M. *J. Synchrotron Radiat.* **2005**, *12*, 537–541.
(20) D'Angelo, P.; Pacello, F.; Mancini, G.; Proux, O.; Hazemann, J. L.; Desideri, A.; Battistoni, A. *Biochemistry* **2005**, *44*, 13144–13150.
(21) Rehr, J. J.; Mustre de Leon, J.; Zabinsky, S. I.; Albers, R. C. *J. Am. Chem. Soc.* **1991**, *113*, 5135–5140.
(22) Bruno, I. J.; Cole, J. C.; Edgington, P. R.; Kessler, M.; Macrae, C. F.; McCabe, P.; Pearson, J.; Taylor, R. *Acta Crystallogr. B* **2002**, *58*, 389–397.
(23) Markley, J. L.; Bax, A.; Arata, Y.; Hilbers, C. W.; Kaptein, R.; Sykes, B. D.; Wright, P. E.; Wuthrich, K. *J. Biomol. NMR* **1998**, *12*, 1–23.

Aliphatic carbon and proton side chain resonances were assigned using three triple-resonance experiments [H(C)CONH-TOCSY, (H)CCONH-TOCSY, and HCCH-TOCSY]. Aromatic proton resonance assignments were obtained from a 2D NOESY experiment acquired in D_2O with unlabeled protein dissolved in 50 mM potassium phosphate buffer, pH 6.8. Standard pulse sequences were taken from the Varian Biopack pulse sequence library.

NMR distance restraints were derived from 3D ^{15}N-edited NOESY−HSQC, 3D ^{13}C-edited NOESY−HSQC, and 3D methyl selective NOESY−HSQC experiments[24] as well as from the 2D-NOESY experiments acquired in D_2O. The following NOE mixing times were used: 140 ms (^{13}C-edited NOESY−HSQC), 100 ms (^{15}N-edited NOESY−HSQC and 2D-NOESY experiments), and 160 ms (3D methyl selective NOESY−HSQC).

For the identification of the metal−ligands, ^{1}H,^{13}C-CT-HSQC and ^{1}H,^{15}N-HMQC experiments, the latter designed for the detection of $^{2}J_{HN}$-couplings in imidazole rings,[25] were acquired. Sequence specific assignments were obtained from the careful analysis of ^{13}C-edited NOESY−HSQC experiments.

All NMR spectra were processed and analyzed using NMRPipe[26] and NMRView.[27,28]

NOE Assignment and Structure Calculation of Cu(I)−CopK. Automatic peak picking and NOE assignment were performed using the UNIO08 software[29,30] and the Cyana molecular dynamics algorithm.[30,31] Talos-derived[32] dihedral restraints together with long-range distance restraints, calculated from manually assigned NOE's involving methyl and aromatic side chain protons, were used as additional input data. The Cu(I) ion was introduced as described in the Cyana manual and connected by a linker consisting of 13 dummy linker residues. Structures were refined using CNS[33] with the distance restraints obtained from UNIO08 together with the Talos-derived dihedral restraints. From an ensemble of 1000 structures, the 50 structures with the lowest total energy were selected and further refined in explicit water. For the CNS calculations, a patched residue was constructed that defined the geometry of the Cu(I) binding site with bond lengths of 2.31 Å between the methionine S atoms and the Cu(I) ion, according to the results of the EXAFS spectroscopy. The force constant used was 1000 kcal mol^{-1} Å^{-2}. No experimental information was available on the S−Cu−S and C−S−Cu bond angles. They were set to 110°, corresponding to a tetrahedral Cu(I) site but restrained with a force constant of only 100 and 70 kcal mol^{-1} deg^{-2}, respectively. The protocol used for the construction of this patched residue is given in the Supporting Information. The representative structural ensemble is formed by the 20 structures with the lowest total energy from the water-refined ensemble. Control structure calculations have been performed without the Cu(I) and the patched residue using an identical CNS protocol.

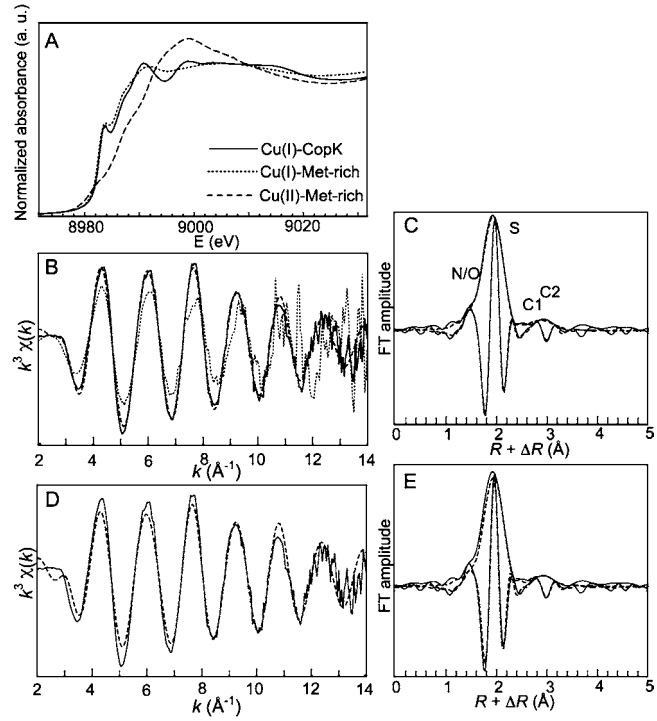

Figure 1. XAS data for Cu(I)−CopK. (A) K-edge XANES spectra for Cu(I)−CopK and Cu(I)−Met-rich and Cu(II)−Met-rich references.[20] (B and D) k^3-weighted EXAFS spectrum for Cu(I)−CopK (solid line, experimental; dashed line, simulation) and for Cu(I)−Met-rich reference (dotted line in B). (C and E) Fourier transform (modulus and imaginary part, non-phase-shift-corrected) for Cu(I)−CopK (experimental) and simulation (dotted lines). Simulations in B and C correspond to the best fit, obtained with 3.8 S and 0.2 N/O atoms in the first shell and two carbon shells (Fit 1 in Table 1) and those in D and E to the fit with 2.8 S and 0.2 N/O atoms in the first shell and two carbon shells (fit 2 in Table 1).

Data Deposition. Chemical shift assignments and molecular coordinates have been deposited with the BioMagResBank (www.bmrb.wisc.edu) under the accession number 16408 and the Protein Data Bank (www.pdb.org) under the accession number 2km0.

Results and Discussion

Spectroscopic Characterization of the Cu(I) Binding Site. Calculating the structure of a metal-bound protein from NMR data requires prior identification of the metal ligands. In the case of Cu(I)−CopK, the Cu(I) site was characterized using XAS and NMR data that were acquired on protein samples of nearly identical composition. On the basis of the observation of chemical shift differences between apo-CopK and Cu(I)−CopK, we had previously proposed a methionine-only coordination involving three of the seven methionines present in the CopK sequence.[13]

XAS. Figure 1A compares the XANES spectra for Cu(I)−CopK with Cu(I)−Met-rich and Cu(II)−Met-rich peptides (KMDT-MSKDMMSME), in which Cu(I) is bound to three S atoms and Cu(II) to four O/N atoms.[20] The spectrum for Cu(I)−CopK presents a pre-edge at 8984 eV attributed to a 1s → 4p transition and characteristic of Cu(I) complexes.[34] Despite the similarity between Cu(I)−CopK and Cu(I)−Met-rich spectra, one cannot conclude on a 3-fold coordination for Cu(I) in Cu(I)−CopK, as the low symmetry around the absorber and the effects of

(24) Van Melckebeke, H.; Simorre, J. P.; Brutscher, B. *J. Am. Chem. Soc.* **2004**, *126*, 9584–9591.
(25) Pelton, J. G.; Torchia, D. A.; Meadow, N. D.; Roseman, S. *Protein Sci.* **1993**, *2*, 543–558.
(26) Delaglio, F.; Grzesiek, S.; Vuister, G. W.; Zhu, G.; Pfeifer, J.; Bax, A. *J. Biomol. NMR* **1995**, *6*, 277–293.
(27) Johnson, B. A.; Blevins, R. A. *J. Biomol. NMR* **1994**, *4*, 603–614.
(28) Johnson, B. A. *Methods Mol. Biol.* **2004**, *278*, 313–352.
(29) Herrmann, T.; Guntert, P.; Wuthrich, K. *J. Biomol. NMR* **2002**, *24*, 171–189.
(30) Herrmann, T.; Guntert, P.; Wuthrich, K. *J. Mol. Biol.* **2002**, *319*, 209–227.
(31) Guntert, P.; Mumenthaler, C.; Wuthrich, K. *J. Mol. Biol.* **1997**, *273*, 283–298.
(32) Cornilescu, G.; Delaglio, F.; Bax, A. *J. Biomol. NMR* **1999**, *13*, 289–302.
(33) Brunger, A. T.; Adams, P. D.; Clore, G. M.; DeLano, W. L.; Gros, P.; Grosse-Kunstleve, R. W.; Jiang, J. S.; Kuszewski, J.; Nilges, M.; Pannu, N. S.; Read, R. J.; Rice, L. M.; Simonson, T.; Warren, G. L. *Acta Crystallogr. D Biol. Crystallogr.* **1998**, *54*, 905–921.
(34) Kau, L. S.; Spira-Solomon, D. J.; Penner-Hahn, J. E.; Hodgson, K. O.; Solomon, E. I. *J. Am. Chem. Soc.* **1987**, *109*, 6433–6442.

Table 1. Structural Environment for Cu in Cu(I)−CopK Obtained from EXAFS Data Analysis[a]

Cu(I)−CopK	atom	*N*	*R* (Å)	σ^2(Å^2)	*R* factor
fit 1: $N_S + N_{N/O} = 4$	S	3.8	2.31	0.0056	0.4×10^{-2}
	N/O	0.2	1.92	0.0035	
	C1	1.1	3.12	0.0070	
	C2	4.7	3.35	0.0070	
fit 2: $N_S + N_{N/O} = 3$	S	2.8	2.31	0.0038	1.8×10^{-2}
	N/O	0.2	1.92	0.0035	
	C1	1.6	3.12	0.0070	
	C2	5.1	3.35	0.0070	

[a] *N*, number of atoms; *R*, interatomic distance; σ^2, Debye−Waller factor; *R* factor, residual between fit and experiment. C1 and C2 refer to the first and second carbon shell, respectively. The following constraints on the parameters were applied: $N_{N/O} + N_S = 4$; σ^2 for the C shells were set equal.

multiple scattering preclude the unambiguous interpretation of the XANES spectrum. Indeed, the coordination chemistry of Cu(I) is very complex and the relation between the XANES features and coordination is not fully understood. This is suggested by the variability of published spectra of Cu(I)−4S sites in terms of peak position and intensities,[34–36] and to our knowledge, there is only one example of a Cu(I) ion coordinated by four sulfur atoms in a protein.[35] This protein contains a (MoS_2CuS_2Mo) cluster, with an average Cu−S distance of 2.305 Å, and the corresponding Cu K-edge XANES spectrum is relatively similar to the Cu(I)−CopK spectrum with a peak at about 8983 eV, a shoulder at 8986 eV, and a peak at 8989 eV.[35]

EXAFS spectra also provide information on coordination number and interatomic distances between the absorber and surrounding atoms in the ligand shell. Figure 1B compares the EXAFS spectrum for Cu(I)−CopK and for Cu(I)−Met-rich peptide. The former has a clearly higher amplitude than the latter, in which Cu(I) is bound to three S atoms. The Fourier transformed EXAFS spectrum for Cu(I)−CopK shows that the first peak is centered at $R + \Delta R = 1.9$ Å, a distance characteristic of S neighbors, with a small shoulder at $R + \Delta R = 1.5$ Å (Figure 1C). This peak was correctly simulated by 3.8 S atoms at 2.31 Å and 0.2 N/O atoms at 1.92 Å. The second peak centered at $R + \Delta R = 2.9$ Å is relatively broad and of small amplitude and could be fitted with two carbon shells.

As the XANES spectrum closely resembled the spectrum of the reference compound with Cu(I) in a 3S site, we carefully examined the validity of the EXAFS simulation. Table 1 compares the fitting results obtained with 3- and 4-fold Cu−S coordination (fits shown in Figure 1B−E). The simulation assuming a 3-fold coordination is clearly weaker with a 4-fold increase of the *R*-factor compared to the 4S coordination. A fit of the first peak only ($R + \Delta R$ range 0.9−2.4 Å) with three and four S atoms showed a similar increase in the residual for the Cu−3S fit (data not shown). Additional support for a Cu(I)−4S site is also provided by the observed Cu−S distance of 2.31 Å. A survey of the CSD database (Figure S1A, Supporting Information) showed that, for small molecules, the Cu−S average distance is 2.26 Å for Cu(I)−3S and 2.33 Å for Cu(I)−4S. The distribution of distances was modeled supposing a Gaussian distribution. The distance of 2.31 Å clearly lies in the full-width at half-maximum (fwhm) of the Cu(I)−4S model, but it does not fall in the fwhm for the Cu(I)−3S model. Nearly identical average distances were found after exclusion of sites belonging to clusters, as these are not representative for the Cu environment in Cu(I)−CopK (Figure S1B, Supporting Information). This survey suggests that the observed distance of 2.31 Å is unusual in trigonal but common in tetrahedral Cu(I)−S sites. Finally, this analysis was restricted to compounds with either thiol (RS) or thioether (RSR) ligands, which are more relevant for the analysis of Cu(I) sites in proteins (Figure S1C, Supporting Information). The CSD database did not contain any structure with a Cu(I)−3(RSR) site. Average distances for Cu(I)−3(RS), Cu(I)−4(RSR), and Cu(I)−4(RS) were 2.26, 2.30, and 2.34 Å. Therefore, the Cu−S distance determined for Cu(I)−CopK is consistent with a tetrathioether environment for Cu(I).

The N/O contribution is relatively small (0.2 N/O for 3.8 S atoms); therefore, the validity of the retained model was checked by wavelet analysis of the spectrum.[37] In particular, we verified that the shoulder on the S peak was not an artifact of the Fourier transformation and that its *k*-space dependency was consistent with O/N atoms (see Figure S2 in the Supporting Information).

The EXAFS parameters indicate that Cu is mostly 4-fold coordinated by S ligands, with a minor proportion bound to O/N ligands. This suggests that Cu(I) occupies two different sites. The first one is composed of four S atoms at 2.31 Å and a C shell (C2 in Table 1) at 3.35 Å and is consistent with Cu(I) bound to the thioether group of four methionine residues. In this site, the number of C2 atoms should be twice the number of S atoms. It is slightly lower, probably due to some interference with other atoms and/or to some structural disorder that attenuates this contribution. The second site contains an O/N shell at 1.92 Å and a C shell at 3.12 Å (C1 in Table 1) and may correspond to a copper ion bound to histidine. This site corresponds to a minor population, and the precision of the parameters does not enable a positive identification of the ligands. From the coordination numbers of the first shell (0.2 O/N atoms and 3.8 S atoms), one can conclude that about 95% of copper occupies the Cu−Met site. The contribution of the second site, that accounts for roughly 5% of the copper ions, may originate from a small amount of Cu(I)Cu(II)−CopK that formed during sample preparation. Indeed, the sample was prepared by adding a small volume of $CuCl_2$ to the protein solution containing 10 mol equiv of sodium ascorbate under air atmosphere, as the manipulation of the sample holder could not be performed in a glovebox. It has previously been shown that binding of Cu(I) to CopK increases its affinity for Cu(II).[14] Under our experimental conditions, we can assume a competition between reduction of Cu(II) to Cu(I) and Cu(II) binding by Cu(I)−CopK. However, the Cu(I)−CopK species remains largely predominant.

Identification of Cu(I) Ligands by NMR Spectroscopy. NMR chemical shifts are very sensitive probes of the chemical environment of a given nucleus. As already shown in numerous cases, significant backbone chemical shift variations are detected for residues that are situated in or close to metal sites.[15–17,38,39] However, this generally does not allow the unambiguous identification of those residues that are directly involved in the

(35) George, G. N.; Pickering, I. J.; Yu, E. Y.; Prince, R. C.; Bursakov, S. A.; Gavel, O. Y.; Moura, I.; Moura, J. J. G. *J. Am. Chem. Soc.* **2000**, *122*, 8321–8322.
(36) Poger, D.; Fillaux, C.; Miras, R.; Crouzy, S.; Delangle, P.; Mintz, E.; Den Auwer, C.; Ferrand, M. *J. Biol. Inorg. Chem.* **2008**, *13*, 1239–1248.
(37) Muñoz, M.; Argoul, P.; Farges, F. *Am. Mineral.* **2003**, *88*, 694–700.
(38) Arnesano, F.; Banci, L.; Bertini, I.; Mangani, S.; Thompsett, A. R. *Proc. Natl. Acad. Sci. U.S.A.* **2003**, *100*, 3814–3819.
(39) Rossy, E.; Champier, L.; Bersch, B.; Brutscher, B.; Blackledge, M.; Coves, J. *J Biol Inorg Chem* **2004**, *9*, 49–58.

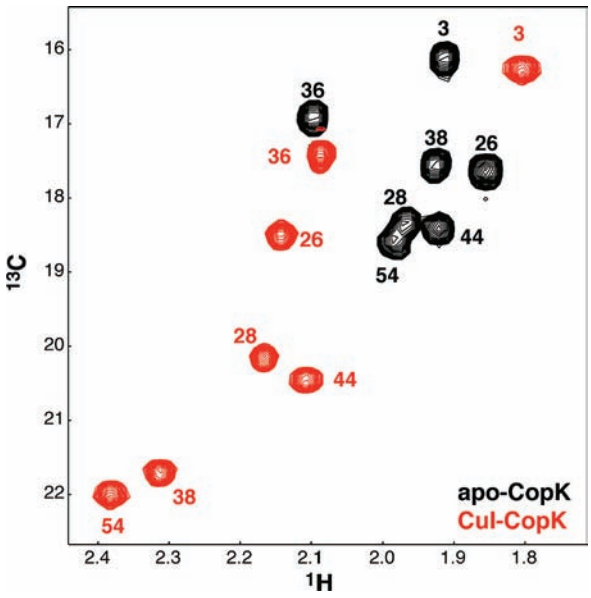

Figure 2. Identification of Cu(I)-coordinated methionine residues by NMR. ^{1}H,^{13}C-HSQC spectra of apo-CopK (black) and Cu(I)−CopK (red) focused on Met-C$^{\varepsilon}$ correlations. Note the significant downfield shift in the ^{13}C-dimension for four of the seven methionines.

metal binding site. We have shown previously that none of the two histidines of CopK was involved in Cu(I) binding and suggested a methionine-only Cu(I) site. Direct identification of Cu(I)-bound methionines from NMR data other than backbone chemical shifts has never been reported in the literature. Comparing the ^{1}H,^{13}C-HSQC spectra for apo-CopK and Cu(I)−CopK, we noticed significant downfield shifts of four methionine methyl carbon resonances (Met-C$^{\varepsilon}$) that were characterized by chemical shifts >20 ppm (Figure 2). Statistical analysis of the chemical shift data provided by the BMRB showed that the chemical shift of Met-C$^{\varepsilon}$ is expected at 17.17 ± 1.96 ppm. Only 2.9% of Met-C$^{\varepsilon}$ chemical shifts reported had values >20 ppm; this also includes shifts measured on paramagnetic proteins. In the case of the CopK protein, the concomitant observation of the downfield shift of four Met-C$^{\varepsilon}$ (M28, M38, M44, and M54) and the fit of the EXAFS data to a Cu(I) ligand shell composed of four sulfur atoms strongly suggests that the chemical shift of this methyl carbon probes the presence of a copper ion bound to the methionine S$^{\delta}$ atom. The same observation was reproduced on a second Cu(I)-binding protein, a CusF-like protein containing a Cu(I)/Ag(I) site identical to that of CusF, formed by two methionines and one histidine.[40,41] On this protein, the Met-C$^{\varepsilon}$ resonance frequencies of the two methionines known to bind copper shifted to values above 20 ppm upon interaction with Cu(I) (see Figure S3 in the Supporting Information). Met-C$^{\varepsilon}$ resonances are easily detectable in constant time ^{1}H,^{13}C-HSQC spectra: they show a high signal-to-noise ratio and can be separated from other methyl groups due to their particular proton chemical shift and their opposite sign. On the basis of our experimental results, we propose that the chemical shift of these carbons provides a new and interesting probe for the detection of methionine-bound Cu(I) and allows the sequence-specific identification of the Cu(I) ligands.

EXAFS and NMR data strongly suggest that CopK coordinates Cu(I) in a tetrathioether metal site. So far, there is only one description of a Cu(I) ion coordinated by four S atoms in a copper chaperon: in crystals of the low-pH form of dimeric CopC, Cu(I) was bound by four methionines provided by the two protein chains, with an average Cu−S distance of 2.3 Å.[42] However, the crystal structure obtained at pH 7.5 and XAS data indicate a S$_n$/N coordination for Cu(I) in the same protein, with n varying between 1 and 3.[38,42] CopK can therefore be considered as the first methionine-rich periplasmic protein with a tetrathioether−Cu(I) site.

Solution Structure of Cu(I)−CopK. Combined use of the EXAFS and chemical shift data described above provided essential experimental information on the geometry of the Cu(I) binding site. On the basis of the ^{1}H,^{13}C-HSQC spectra, methionines 28, 38, 44, and 54 were identified as Cu(I) ligands. The Cu−S distance determined to be 2.31 Å from the fits of the EXAFS spectra was introduced in the structure calculations either as an experimental distance (CYANA calculations) or as the Cu−S bond length in the patched residue, composed of the four methionines and the copper ion (CNS calculations; see Supporting Information for a detailed description of the patched residue).

Figure 3 shows the final structural ensemble of Cu(I)−CopK comprising 20 structures. Structural statistics are given in Table S1 (Supporting Information). The structure is well-defined with a mean backbone rmsd of 0.61 Å and is composed of two β-sheets. The Cu(I) ion is situated in a tetrahedral binding site (S−Cu−S angles of 109.4° ± 2.6°) and is located between the two β-sheets with its ligands provided by the N-terminal β-sheet (M28), the loop connecting the two β-sheets (M38), and the C-terminal β-sheet (M44, M54). Figure 4 shows the comparison of Cu(I)−CopK and apo-CopK solution structures. Whereas the topology of the protein core seems to be nearly unchanged (backbone atoms of residues 6−54 can be superimposed with an rmsd of 1.7 Å), there are striking differences between the two structures: the C-terminal β-sheet lacks the last strand, which appears disordered in the metal-bound form, and the unstructured C-terminal part has a completely different orientation.

Partial disruption of the C-terminal β-sheet in Cu(I)−CopK can experimentally be demonstrated by the analysis of the backbone chemical shifts (see Figure S4, Supporting Information) and also by the very weak ^{1}H,^{15}N-correlations in the HSQC spectrum.[13] In addition, experimental data previously reported for apo-CopK[13] indicate a local increase in flexibility in the part of the protein undergoing this large conformational modification upon Cu(I) binding. Hydrogen exchange measurements have demonstrated that the amide protons involved in hydrogen bonds connecting the last two β-strands of the C-terminal sheet exchange more rapidly with the solvent than those situated in other interstrand hydrogen bonds.[13] Figure S5 in the Supporting Information shows the free energy changes for structural opening calculated from solvent exchange rates mapped on the solution structure of apo-CopK. In addition, N57, which drastically changes its backbone conformation from ϕ/ψ = 60°/10° in the apo-form (ϕ/ψ = 59°/25° in the crystal structure of apo-CopK[14]) to ϕ/ψ = −60/−10 in Cu(I)−CopK, showed an increased transverse ^{15}N-relaxation rate in apo-CopK. This residue can be considered as the hinge for the reorientation of the C-terminus due to copper binding. The increased

(40) Loftin, I. R.; Franke, S.; Blackburn, N. J.; McEvoy, M. M. *Protein Sci.* **2007**, *16*, 2287–2293.
(41) Xue, Y.; Davis, A. V.; Balakrishnan, G.; Stasser, J. P.; Staehlin, B. M.; Focia, P.; Spiro, T. G.; Penner-Hahn, J. E.; O'Halloran, T. V. *Nat. Chem. Biol.* **2008**, *4*, 107–109.
(42) Zhang, L.; Koay, M.; Maher, M. J.; Xiao, Z.; Wedd, A. G. *J. Am. Chem. Soc.* **2006**, *128*, 5834–5850.

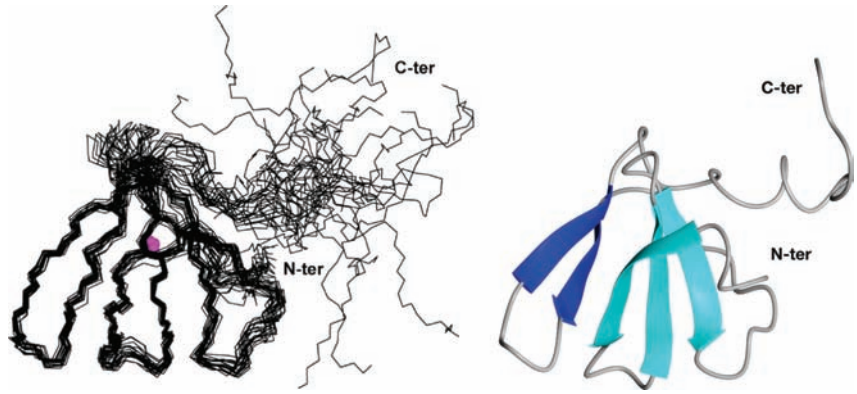

Figure 3. Solution structure of Cu(I)−CopK. (Left) Structural ensemble of 20 structures. The Cu(I) ion is shown in magenta. (Right) Ribbon diagram of the representative Cu(I)−CopK structure; N- and C-terminal β-sheets are shown in cyan and in blue, respectively.

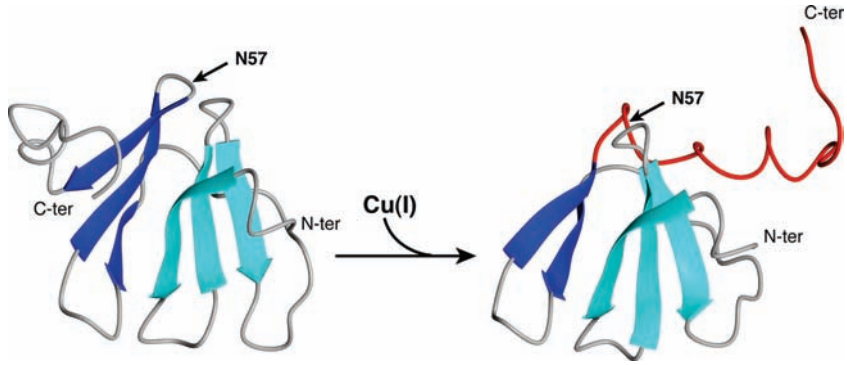

Figure 4. Structural modifications upon Cu(I) binding: comparison of apo-CopK and Cu(I)−CopK. Representative structures of apo-CopK (left) and Cu(I)−CopK (right) in ribbon representation. Note the disruption of the C-terminal β-sheet and the reorientation of the C-terminal tail, shown in red in the Cu(I)−CopK structure. The hinge residue N57 is indicated.

conformational exchange of N57 and the lower stability of the hydrogen bonds between the two C-terminal β-strands suggest that the inherent structural flexibility required for the conformational reorientation of the C-terminus may be pre-encoded in the apo-form of CopK.

We and others[13,14] have previously shown that apo-CopK dimerizes with a dissociation constant of 5×10^{-5} M, whereas Cu(I)−CopK is monomeric in solution, even at millimolar concentration. This observation can be rationalized when considering that upon Cu(I) binding the last strand of the C-terminal β-sheet, which forms the dimer interface, breaks apart. Even more importantly, the global movement of the C-terminus can be correlated to the formation of the Cu(II)-binding site, which probably involves H70. This residue appears to be conserved in the C-terminal part of the CopK-like proteins (see sequence alignment in the Supporting Information) and its backbone resonances have been shown to disappear after Cu(II) binding.[14] We did not attempt to better define the Cu(II) binding site in Cu(I)Cu(II)−CopK because of the limited quality of the spectra and numerous missing resonances that are due to the presence of the paramagnetic Cu(II) ion. However, a $^{1}H,^{15}N$-HMQC spectrum designed for the detection of $^{2}J_{HN}$-couplings in imidazole rings did not reveal any signal, suggesting that both histidine side chains are within 11 Å of the Cu(II) ion (data not shown). In apo-CopK, the two histidine side chains are separated by more than 15 Å.

Structure calculations performed in absence of the Cu(I) ion but with identical experimental restraints converged to the same structure with an rmsd of 0.72 Å (backbone atoms of residues 2−54) between the mean structure of the control ensemble and the representative Cu(I)−CopK structure.

Comparison with the X-ray Structure of Copper-Bound CopK and Implications for Cooperative Cu(I)/Cu(II) Binding. Recently, Chong and co-workers determined the X-ray structures of apo- and copper-bound CopK.[14] In both cases, they observed that the crystal was composed of protein dimers, independently of whether copper was present or not. The crystal structures of apo-CopK and Cu(I)−CopK were found to be conformationally identical and the backbone atoms could be superposed to the apo-CopK solution structure with rmsd values of 0.98 and 1.05 Å, respectively. The crystal structure of metal-bound CopK contained a single Cu(I) ion, despite the fact that crystals were grown from preparations of Cu(I)Cu(II)−CopK. In this structure, the metal was coordinated to three methionine residues, M26, M38, and M54.[14] The authors explained the dimeric structure of the Cu(I)-bound protein in the crystal structure, which was otherwise shown to be monomeric in solution,[13,14] by strong intermolecular hydrogen bonds and the high protein concentration in the crystal.

Comparison with the solution structure of Cu(I)−CopK described here reveals not only significant differences in the structure of the C-terminal part, but also in the Cu(I) coordination. Indeed, in the crystal structure, different methionine residues form the Cu(I) site, as shown in Figure 5. We have shown that in the Cu(I)−CopK solution structure Cu(I) is coordinated to four methionines (M28, M38, M44, and M54), whereas the copper ion is bound by three methionines (M26, M38, and M54) in the crystal structure. Therefore, the solution structure of Cu(I)−CopK determined under reducing conditions

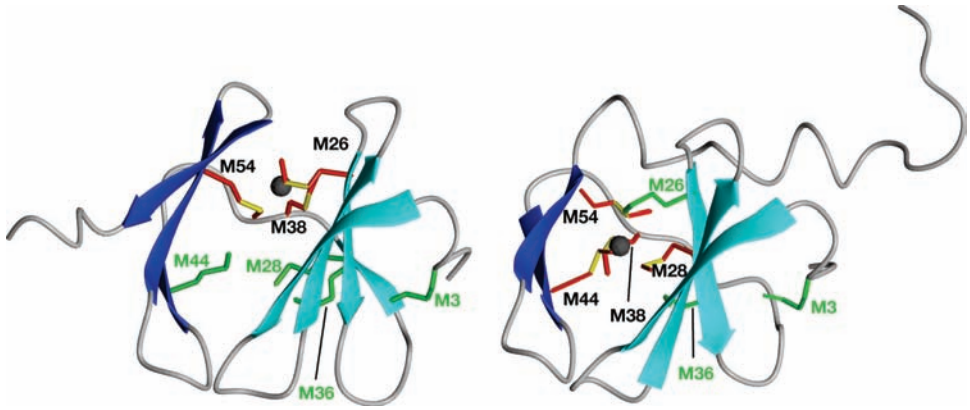

Figure 5. The Cu(I) binding sites in CopK. Comparison of the X-ray structure of Cu(I)−CopK (left) with the solution structure of Cu(I)−CopK (right). Methionine side chains involved in Cu(I) coordination are shown in red with the bond connecting the C^{γ} and the sulfur atoms in yellow. The remaining methionines are given in green. Note that only one subunit of the Cu(I)−CopK dimer is shown in case of the crystal structure.

Scheme 1. Molecular Basis for Cooperative Cu(I)/Cu(II) Binding of CopK

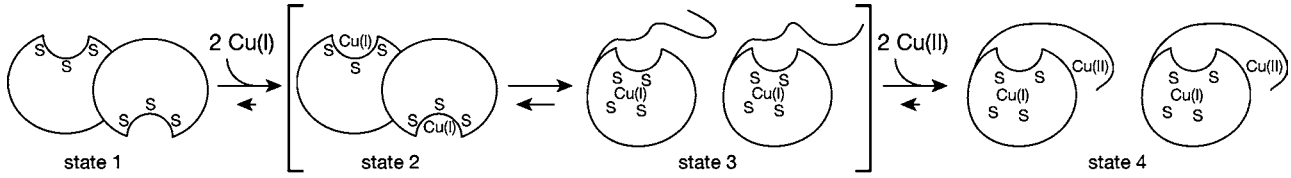

and the crystal structure of Cu(I)−CopK obtained from Cu(I)Cu(II)−CopK by Chong et al. represent two different forms of the Cu(I)-bound protein.

NMR experiments acquired on Cu(I)−CopK provide experimental evidence that, in solution, Cu(I)−CopK populates two different states. Numerous residues are characterized by broad lines in the $^{1}H,^{15}N$-HSQC spectrum (7, 18, 29, 55−62) or show increased ^{15}N transverse relaxation rates (8, 10, 19, 27, 30, 52, and 53; see Figure 8c in ref 13 and Figure S6 in the Supporting Information). The major population is represented by the solution structure determined here, whereas the minor one is only detectable via the increases in transverse relaxation rates. Many of the residues for which increased ^{15}N transverse relaxation has been observed are situated in the last two strands of the C-terminal β-sheet in apo-CopK (residues 52, 53, 55−62), where the large conformational change occurs upon Cu(I) binding. It is therefore reasonable to assume that the minor conformation contains a three-stranded C-terminal β-sheet as observed for apo-CopK or for the crystal structure of Cu(I)−CopK. The dissociation constant for Cu(I) has been determined to be in the range of 10^{-11} M for apo-CopK,[14] which suggests that under NMR conditions the equilibrium is completely displaced toward Cu(I)−CopK. Therefore, it is unlikely that the observed chemical exchange results from an equilibrium between Cu(I)−CopK and apo-CopK.

Alternatively, the minor form may correspond to the crystal structure of Cu(I)−CopK that became trapped during crystallization of Cu(I)Cu(II)−CopK.[14] Assuming that the major form of Cu(I)−CopK is less prone to crystallization because of the larger number of flexible residues, an equilibrium between the two described Cu(I)−CopK structures in solution could lead to the crystallization of the minor form. Additional support for the physiological relevance of both Cu(I)-bound forms is provided by primary sequence analysis. Indeed, sequence alignment of *C. metallidurans* CH34 CopK with other CopK-like proteins reveals that, of the seven methionines present in CopK, five are conserved: M26, M28, M38, M44, and M54 (see Figure S7, Supporting Information) suggesting an important role for all of them. These five methionines correspond exactly to the ensemble of the methionine ligands observed in the two different Cu(I)−CopK structures (see Figure 5), underlining that both metal sites may be populated in the different states of CopK.

On the basis of this analysis, we propose that the Cu(I)−CopK X-ray structure may correspond to a first encounter complex between CopK and Cu(I). In this complex, Cu(I) interacts with M26, M38, and M54, which form a single patch at the protein surface. The formation of this initial complex does not trigger the reorientation of the C-terminal part related to dimer dissociation and formation of the Cu(II) site. In a second step, the Cu(I) ion migrates to a second site, described by the solution structure presented here, in which it is coordinated to four sulfur atoms. It can be imagined that this is directly related to the molecular motion around N57, leading to the reorientation of the C-terminal tail. At high protein concentrations, this is associated with dimer dissociation, as the dimer interface involves the C-terminal β-sheet and leads to the formation of the Cu(II) site. Cu(II) binding would then stabilize the protein in a fourth state that corresponds to the air-stable Cu(I)Cu(II)−CopK described by Chong et al.[14] with an increased Cu(I) affinity of Cu(I)Cu(II)−CopK with respect to Cu(I)−CopK. The $^{1}H,^{13}C$-HSQC spectrum acquired for Cu(I)Cu(II)−CopK shows that Cu(I) remains coordinated to M38, M44, and M54 after binding of Cu(II) in its specific site. The $^{1}H,^{13}C$-correlation peak for M28 shifts back to <20 ppm at an intermediate position between an apo and Cu(I)-bound state and has a much weaker amplitude (see Figure S8, Supporting Information). This may either indicate internal dynamics with a partial participation of M28 in Cu(I) binding and/or relaxation by the nearby Cu(II) ion. The overall reaction of CopK with Cu(I) and Cu(II) can therefore be described by four states, as summarized in Scheme 1, with states 2 and 3 having a very short lifetime in the oxidizing environment of the periplasm.

It is interesting to note that CopK is another periplasmic copper protein that simultaneously binds Cu(I) and Cu(II). Other examples are the CopC/PcoC copper chaperon[38,42,43] and the CzcE protein from *C. metallidurans* CH34 that has recently been characterized.[44] For these proteins, it has been observed that the Cu(I)-bound forms were sensitive to oxidation, whereas the Cu(I)Cu(II) proteins were air-stable.[14,42,44] Therefore, it may be proposed that the presence of Cu(II) helps to stabilize protein-bound Cu(I) in the oxidizing environment of the periplasm. CopK is the first protein for which a Cu(I)/Cu(II)-binding cooperativity has been observed that we propose to be related to a significant structural modification occurring upon binding of a first Cu(I) ion to CopK. Compared to the other two proteins, CopK is unique, as it only binds Cu(II) in presence of Cu(I). This indicates that CopK is involved in the Cu(I) detoxification of the periplasm by a mechanism that may differ from that of CopC/PcoC.

Conclusion

We have determined the solution structure of Cu(I)−CopK. Spectroscopic investigation of the Cu(I) site by XAS revealed that Cu(I) is bound to four methionine thioether groups. To our knowledge, this is the first example of a XANES and EXAFS characterization of a tetrathioether Cu(I) site in a protein that is not part of a CuS cluster. Using NMR spectroscopy, a characteristic downfield shift of the Met-C$^{\varepsilon}$ resonance frequency visualized in a CT-^{1}H,^{13}C-HSQC spectrum allowed identification of the methionine residues involved in Cu(I) coordination. We propose that the Met-C$^{\varepsilon}$ chemical shift provides a new and interesting probe for the identification of Cu(I)-bound methionines.

Analysis of the Cu(I)−CopK solution structure provides significant information for the understanding of the observed Cu(I)/Cu(II) binding cooperativity. We demonstrate that accommodation of Cu(I) in the tetrathioether site is associated with an important structural modification of the C-terminal part of the protein: partial disruption of the C-terminal β-sheet results in a 180° rotation of the C-terminal tail (residues 55−74) with N57 as the hinge. This also modifies the protein surface involved in the dimer interface, resulting in the formation of monomeric Cu(I)−CopK. We propose that this reorientation is required for the formation of the Cu(II)-specific site and can therefore be considered as the missing link between the X-ray and solution structures characterized so far[13,14] and the observed binding cooperativity between Cu(I) and Cu(II).

Acknowledgment. We are very grateful to Isabel Ayala for protein purification. We thank the ESRF for the provision of beamtime and the staff of the FAME beamline and Florian Molton (LGIT) for their assistance during XAS data acquisition. We also thank Manuel Muñoz for the wavelet analysis and Yves Joly for stimulating discussions on the XANES spectra. The Commissariat à l'Energie Atomique, the Centre National de la Recherche Scientifique, the Université Joseph Fourier, and the French program Tox-Nuc-E are acknowledged for financial support.

Supporting Information Available: Protocol for the generation of the patched Cu(Met)$_4$ residue; Table S1 resuming the structural statistics of the NMR ensemble; and Figures S1−S8 presenting the distribution of Cu−S distances in 4S−Cu(I) and 3S−Cu(I) sites, the wavelet analysis of the EXAFS spectrum, the sequence alignment of CopK-like proteins, ^{1}H,^{13}C-HSQC spectra of Cu(I)Cu(II)−CopK and of a CusF-like protein, NMR data related to the structural change between apo-CopK and Cu(I)−CopK, and mapping of residues with an increased exchange contributions to the transverse relaxation rates on the 3D structure of Cu(I)−CopK. This material is available free of charge via the Internet at http://pubs.acs.org.

JA9083896

(43) Djoko, K. Y.; Xiao, Z.; Huffman, D. L.; Wedd, A. G. *Inorg. Chem.* **2007**, *46*, 4560–4568.
(44) Zoropogui, A.; Gambarelli, S.; Coves, J. *Biochem. Biophys. Res. Commun.* **2008**, *365*, 735–739.